Micro-Propulsion Concepts Utilizing Microplasma Generators

Kunning G. Xu[1]
University of Alabama in Huntsville, Huntsville, AL, 35899, USA

A small-scale microplasma source is being built to function as a space propulsion device. An overview of microplasma sources is presented followed by current research in microplasma thrusters. A simple analysis of the different acceleration mechanisms (electrothermal, electrostatic, and electromagnetic) is performed based on the design of a microwave microstrip microplasma thruster. Performance calculations, where possible, and practical considerations suggest that electrothermal is the simplest method for microplasma thrusters, but electromagnetic may provide the best performance. Electrostatic acceleration is deemed infeasible due to higher complexity for limited performance gains compared to electrothermal. Electrostatic grids also have potential difficulties in breakdown and charge exchange due to the higher operating pressure of microplasma sources.

I.   Introduction

THE miniaturization of electronics technology has driven similar changes in satellite design. The interest in mini, micro, and nanosats has grown in the last decade. The CubeSat, originally a university teaching tool, has caught the interest of both industry and government. Over 75 CubeSats have been placed in orbit to date. A major drawback of these miniature satellites is the limited space and power available. These limitations typically result in single purpose, short duration missions either due to lack of power or propulsion. The power limitations can be solved with deployable solar panels which are currently under development.[1] The second issue, lack of propulsion, is more difficult but has a wider range of potential solutions. There has been a variety of research in micro propulsion systems ranging from miniature hydrazine thrusters,[2] to solid rockets,[3] and miniature electric propulsion.[4–7] This work investigates micro propulsion possibilities with the use of microplasmas. The research to date in microplasma propulsion has shown good performance for low powers (~1 mN at 5 W). This paper presents an overview of microplasma sources/generators, current microplasma based thrusters, an analysis of different acceleration schemes as applied to a microwave microstrip microplasma thruster (3MT). Section II presents an overview of microplasma sources and some typical plasma properties. Section III discusses the present state of microplasma thruster research and development and provides a brief comparison of current microplasma thrusters to other plasma based micro propulsion systems. Section IV presents a theoretical analysis of the benefits and drawbacks of the various acceleration mechanisms that can be coupled to the proposed 3MT.

II.   Microplasma Sources

Microplasmas are a class of ionized discharges in geometries where at least one dimension is in the millimeter or sub-millimeter range. The reduced dimensions of microplasmas allows them to operate in high-pressure environment according to *pD* scaling, where *p* is the pressure and *D* is the characteristic dimension of the plasma.[8] Microplasmas are characterized by non-equilibrium temperatures,[9,10] non-Maxwellian electron energy distribution functions,[11,12] and high electron densities.[10,13] They are differentiated from corona discharge or dielectric barrier discharges (DBD) by their enforced geometry, though DBD's do form microdischarges in the plasma volume.

The first experiments with microplasmas dates to the 1950's with research into small hollow cathode discharges. White tested a 750 μm diameter hollow cathode and demonstrated normal glow discharge and classic hollow cathode discharge (negative differential resistance).[14] The size of the discharge cavities and thus the upper pressure limit of operation based on *pD* scaling was limited until the 1990's. This was largely due to the growth of microfabrication techniques outside of integrated circuits. Frame *et. al.* fabricated one of the first microdischarge devices in 1997 with at 200 μm diameter cavity on a silicon substrate.[15] Since then, research in the area of

---

microplasmas has grown rapidly, primarily in the materials processing and analytical chemistry communities. The primary benefit of microplasma in those fields is their high-pressure stability that portents non-vacuum materials processing and lab-on-a-chip style chemical analysis. There are many review articles from the last ten years covering the range of research in microplasma from a materials and chemistry perspective.[8,16–18] Numerous devices have been designed and tested from vacuum to atmospheric pressures on a variety of gases.

The range of microplasma source types varies dramatically, however a generalization will be attempted here. Microplasma in various configurations can be excited by DC, pulsed DC, AC, rf, or microwave sources. The average electron temperature is typically low, approximately in the 1-2 eV range, but the electron energy distribution exhibits very non-Maxwellian behavior and can have a high energy population.[19] The electron densities can exceed 5×10^{18} m^{-3} with high power densities of 10^4-10^6 W-cm^{-3}.[17] The gas temperature depends strongly on the working gas and pressure. Rare gases such as argon exhibit low gas temperatures of a few hundred Kelvin at both vacuum and atmospheric conditions, while molecular gases such as air produce high gas temperatures upward of 2000 K at atmospheric conditions. The increase in temperature for molecular gases is likely due to the existence of more internal energy modes compared to atomic gases.

Some examples of microplasma sources are shown in Figure 1. These are one a few of the published sources and include the microcavity device by Eden,[20] the capillary discharge of Shimizu,[21] and the microstrip resonators by Hopwood[22] and Schermer.[23] Applications of microplasma sources include plasma etching,[24] nanoparticle formation,[25] lighting,[26] chemical analysis,[27] tissue engineering,[28] sources of UV and excimer radiation,[29] and propulsion.[30,31]
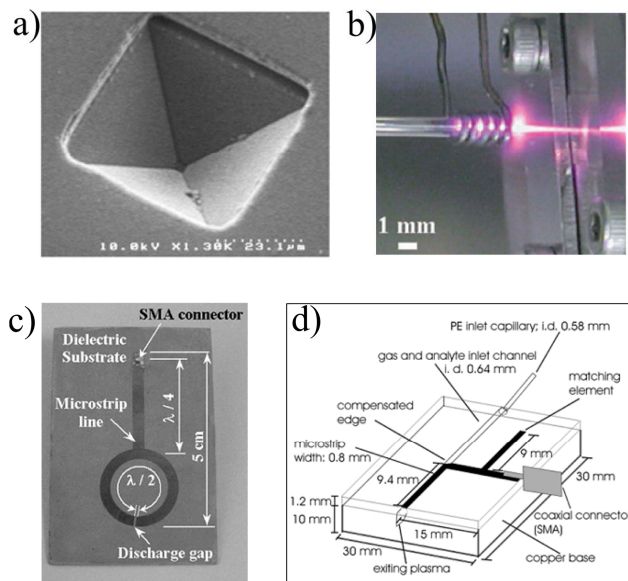

Figure 1. Example microplasma sources: a) microcavity of Eden,[20] b) microcapillary of Shimizu,[21] c) microstrip/split-ring resonator of Hopwood,[22] and d) linear microstrip of Schermer.[23]

III. Current Microplasma Thruster Research

In micro propulsion, the use of microplasma has been focused on microcavity discharges[30,32–35] and microwave excited microplasmas.[31,36] Some authors use the term micro-hollow cathode discharge (MHCD) to describe a microcavity discharge, however this may be slightly misleading. Typically, hollow cathode discharge refers to a specific operational mode in a DC device where voltage decreases as current increase (negative differential resistance). To avoid confusion, we will refer to such devices as microcavity discharges or thrusters. Microcavity thrusters are comprised of a pair of electrodes separated by a dielectric, usually created with deposition or etch techniques. The working gas is ionized and heated through either AC or DC electrical breakdown to form a surface plasma. The plasma and neutral gas is heated to ~1000 K and then accelerated through a micronozzle to produce thrust. Figure 2 shows three examples of microcavity discharge thrusters from Burton,[30] Guangqing,[32] and Tuyen.[35]
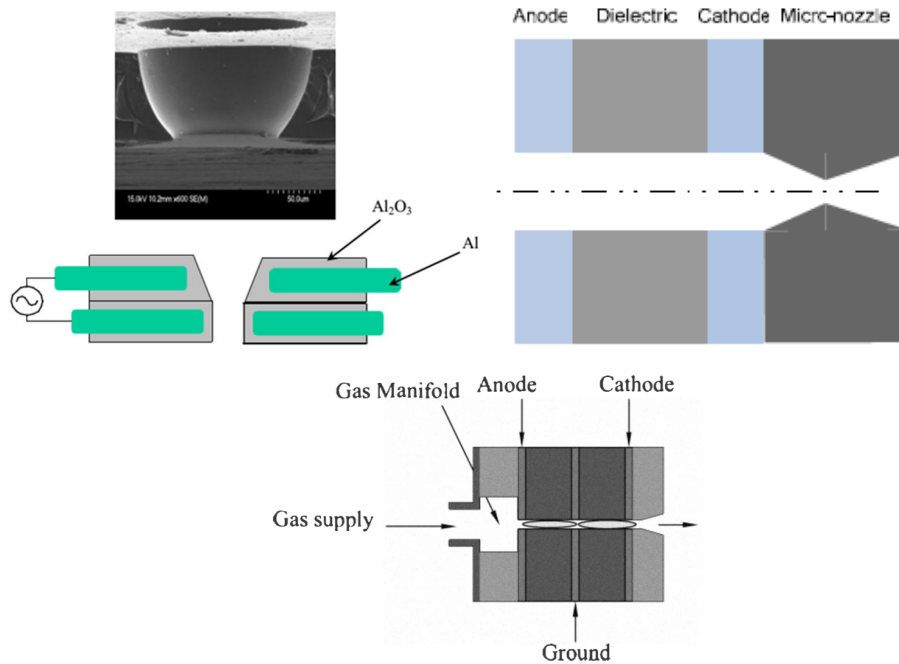
Figure 2. Microcavity discharge thruster with micronozzle from (left) Burton,[30] (right) Guangqing,[32] and (bottom) Tuven.[35]

As there are very few devices tested to date, generalization of their performance is difficult to do. The experimental results so far has shown a single microcavity discharge thruster can generate thrust on the order of 0.5-1 mN with < 5 W of power.[30,32,35] However they can easily be stacked in arrays for higher thrust levels. Hitomi et.al. compared a single microdischarge thruster to a 3x3 array and found the array produced nearly double the thrust per discharge cavity.[33] The maximum thrust obtained with the 3x3 array was 8.6 mN running 11.3 mg/s of argon at 5.4 W discharge power. This is likely due to interactions between the multiple jets and boundary layers resulting in better nozzle expansion and pressure matching.

The microwave microplasma thruster by Kawanabe et. al. shown in Figure 3 also used a micronozzle to accelerate the flow.[36] The difference from the microcavity discharge thruster is the use of microwave excitation.
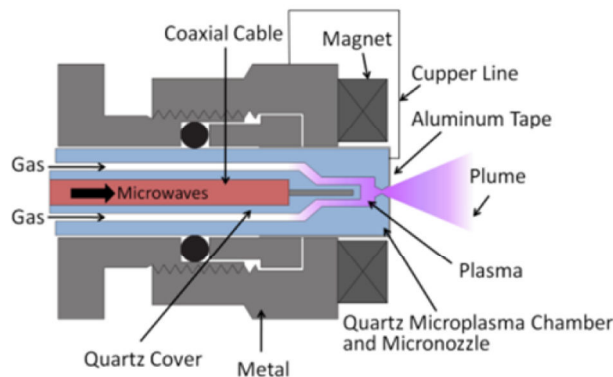

Figure 3. A microwave microplasma thruster with micro nozzle and magnetic field by Kawanabe et. al.[36] The magnetic field is intended to magnetize electrons and increase ionization and thrust.

A coaxial cable propagates the microwave signal to a discharge chamber filled with gas. The chamber is sized to be approximately 1/4 the driving wavelength. The discharge is ignited through the use of a secondary coil, as there is insufficient microwave power to initiate gas breakdown with the coaxial cable alone. After initial ionization, the

3

plasma is sustained by the microwaves. The heated gas flows through a converging-diverging nozzle to produce thrust. The maximum thrust obtained was 1.1 mN running 1.78 mg/s of argon at 6 W of microwave power. Operating at 3 W of power at the same flow rate produced 1 mN of thrust. The thruster was also tested with an axial magnetic field to confine electrons and increase gas heating. The resultant increase in thrust with the magnetic field was less than 12%.[36] The I_{SP} for all cases was less than 70 s.

IV.   Acceleration Analysis for the 3MT

Turning a plasma source/generator into a thruster requires acceleration of the particles. Parallels can be drawn from past work in helicon based thrusters wherein an acceleration method is added to an existing plasma source.[37–39] The current range of microplasma thrusters utilize a converging-diverging nozzle to convert thermal energy into kinetic energy. For the 3MT, as we are building it from the ground up, an opportunity presented itself to analyze the possible acceleration options. Electric propulsion thrusters are generally divided into three categories based on their acceleration mechanism: electrothermal (ET), electrostatic (ES), and electromagnetic (EM). This section presents a basic analysis and discussion of each mechanism as applied to the microstrip microplasma under consideration here for the 3MT.

The 3MT is a microthruster based on the microstrip plasma resonator developed by Bilgic[40] and Hopwood.[22] The 3MT is an extension of the split-ring resonator design by Hopwood that is shown in Figure 4. The microstrip resonator is a microwave driven plasma source easily created with common techniques such as photolithography. The length of the microstrip is set to be an even fraction of the signal wavelength through the dielectric substrate material (e.g., $\lambda/4$ or $\lambda/2$) such that a standing wave is formed. The wavelength of an rf signal through a dielectric is calculated by Eqn. (1)

$$\lambda = \frac{c}{f}\frac{1}{\sqrt{\varepsilon_r}} \ ,$$

(1)

where c is the speed of light, f is the signal frequency, and ε_r is the dielectric constant.
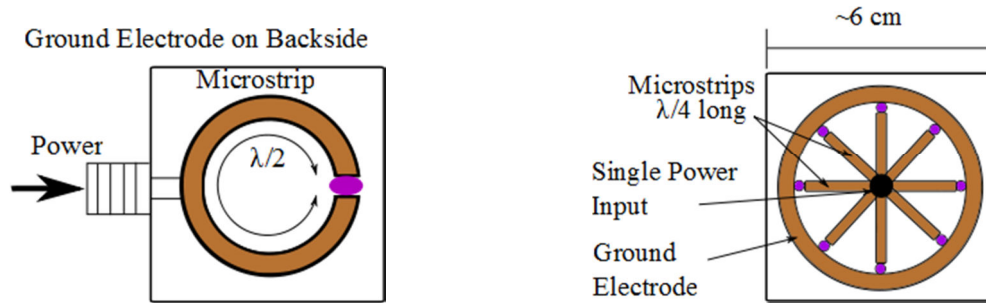

Figure 4. (left) A drawing of the microstrip resonator developed by Hopwood,[22] and (right) a notional drawing of a multi-strip version for use in the 3MT.

A small gap, on the order of 100 μm separates the legs of the microstrip. The amplitude of the rf wave becomes maximized at the gap, resulting in a large electric field. Working gas passed through the gap becomes ionized by the electric field. Electric field values as high as 4 MV/m at only 1 W of power have been calculated for these devices.[41] Microwave frequencies are used to reduce the length of the microstrip and the overall device size. Much of the work on split-ring resonators has been conducted at 900 MHz under 3 W of power. The literature has shown that the resonators are capable of producing plasmas at the micro-scale with little power (~1 W),[42,43] high electron density (~5 x 10^{18} m^{-3}),[43] over a large range of pressures (100 mTorr – 950 Torr),[22,44] and over 24 hours of continuous operation without erosion.[22] The higher density operation of these devices, and in general most microplasma devices has been attributed to the Pendel effect.[45,46] The Pendel effect is when electrons oscillate between the sheath potential regions between the two electrodes. This reduces wall neutralization and greatly increases the effective electron path length, leading to more collisions.

The proposed 3MT is based around a 2D microstrip resonator source shown in the right drawing of Figure 4. The device can be fabricated on a ceramic-Teflon composite with a dielectric constant of 10.2. The microstrips are reduced in length and laid out in a spoke-like fashion surrounded by a ground electrode. Assuming an input frequency of 900 MHz, each microstrip will be 2.6 cm long, thus the entire device would fit on a 6 cm x 6 cm chip. Only eight microstrips are shown for the sake of clarity, but one can imagine dozens or more microstrip spokes. All the microstrips are driven by a single power input to ensure they are in phase. A back plate with an O-ring can be added to create a propellant plenum, and the entire device can be further enclosed to create a plasma volume. Drawings of three potential acceleration designs are shown in Figure 5. The following sub-sections will discuss each design.
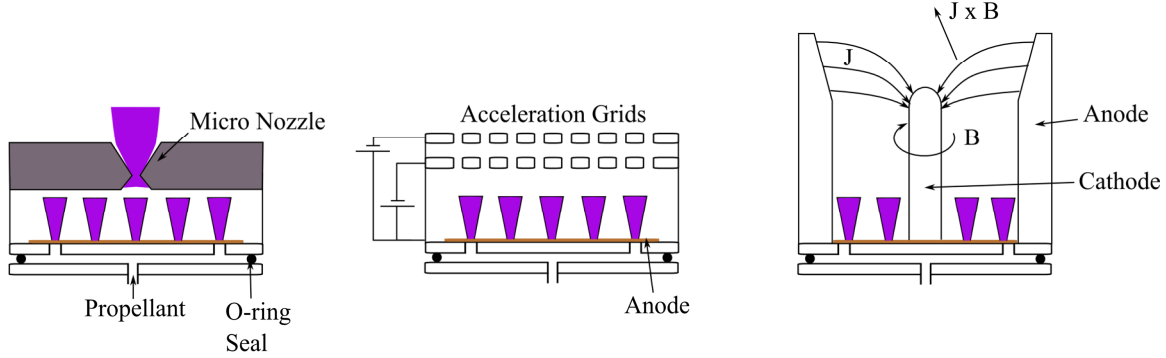
Figure 5. Notional drawings of 3MT with each type of acceleration mechanism: micro nozzle, electrostatic grids, and self-field Lorentz force.

A. Electrothermal

All of the microplasma based thruster concepts to date are of the ET type. A microfabricated converging-diverging nozzle accelerates the gas flow to produce thrust by converting thermal to kinetic energy. This method is well known and used extensively in chemical propulsion. However ET does have performance limits dependent on the gas temperature, pressure, and nozzle expansion ratio. A simple analysis of ET performance can be obtained from the isentropic flow equations for a 1D converging-diverging nozzle summarized in Eqs. (2)-(8).

$$\frac{T_o}{T} = 1 + \frac{\gamma - 1}{2} M^2 \tag{2}$$

$$\frac{p_o}{p} = \left(\frac{T_o}{T} \right)^{\gamma/\gamma - 1} \tag{3}$$

$$\frac{A}{A*} = \frac{\sqrt{\gamma} \left(\frac{\gamma + 1}{2} \right)^{(\gamma+1)/(2-2\gamma)}}{M \sqrt{\gamma} \left(1 + \frac{\gamma - 1}{2} m^2 \right)^{(\gamma+1)/(2-2\gamma)}} \tag{4}$$

$$\dot{m} = \frac{p_o A}{\sqrt{RT_o}} M \sqrt{\gamma} \left(1 + \frac{\gamma - 1}{2} m^2 \right)^{(\gamma+1)/(2-2\gamma)} \tag{5}$$

$$v_e = M_e \sqrt{\gamma RT_e} \tag{6}$$

$$T = \dot{m}v_e + \left(p_e - p_a\right)A_e \tag{7}$$

$$I_{SP} = \frac{T}{\dot{m}g_o} \tag{8}$$

The analysis assumes the plasma can be treated as a calorically perfect gas at the heated temperature, the flow is isentropic and choked at the throat, there is no surface friction or surface heat transfer, and the flow velocity is purely axial. The plasma is assumed to be at a baseline reservoir pressure of 40 kPa (300 Torr) and a gas temperature of 600 K. This is based on laser absorption measurements of a split-ring resonator at 1 W of power.[44] Higher temperatures can be obtained in these devices with higher pressures and power levels. A throat diameter of 100 um is used based on similar micro nozzles in the literature.[30,32,33] Figure 6 shows the thrust and I_{SP} as a function of the exit Mach number. For the given reservoir conditions and a choked flow, the mass flow rate of argon is constant at 0.646 mg/s. At Mach 5, both the thrust and I_{SP} begin to reach an asymptotic value of approximately 0.5 mN and 75 s respectively. The thrust is primarily from momentum thrust, the pressure contribution to thrust in Eq. (7) is negligible.
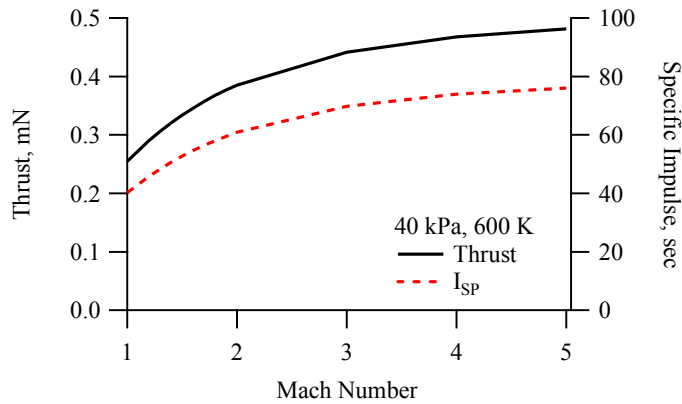
Figure 6. Thrust and specific impulse as a function of nozzle exit Mach number (40 kPa, 600K).

Since these results assume choked and perfectly expanded flow, the thrust becomes insensitive to temperature and the I_{SP} becomes insensitive to reservoir pressure. Figure 7 shows the variation in thrust from 1 – 100 kPa reservoir pressure and Figure 8 shows the variation of I_{SP} from 600 – 2000 K gas temperature. These ranges of pressure and temperature represent demonstrated operating conditions for microplasmas. At the maximum conditions demonstrated to date (atmospheric pressure and ~2000 K), an ET microplasma thruster would produce at best 1.2 mN of thrust at 1400 s of I_{SP}.
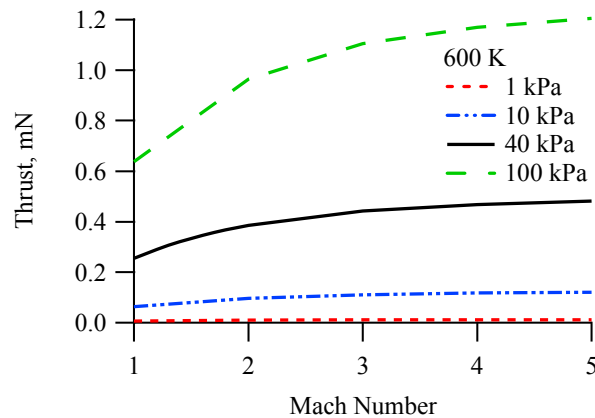
Figure 7. Thrust variation with reservoir pressure. The temperature is held constant at 600 K.
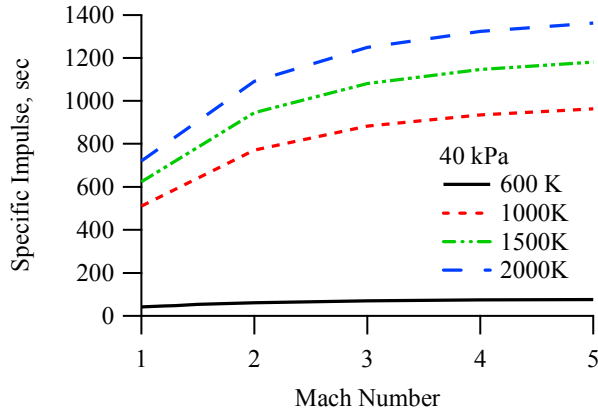
Figure 8. Specific impulse variation with gas temperature. The pressure is constant at 60 kPa.

The microwave microplasma thruster by Takao, later used by Kanawabe, used a micro nozzle to expand a 40 kPa and 1200 K flow at 6 W microwave power. Their work obtained ~0.7 mN of thrust and ~80 s of I_{SP} at a mass flow rate of 30 sccm (0.89 mg/s) of Ar.[47] The conical nozzle was sized to provide an exit Mach number of approximately 8.7. His results were within 5% of the theoretical thrust (0.72 mN) and 40% of the theoretical I_{SP} (111.7 s). This indicates that even the basic idealized equations can provide fair estimates of ET performance for microplasmas.

On the practical side, the primary concern for ET microthruster is the fabrication and lifetime of miniature nozzles. A nozzle size and aspect ratio can be estimated from a conical nozzle given by Eq. (9)

$$\frac{L}{D^*} = \frac{\sqrt{A_e/A^*} - 1}{2\tan\alpha}, \tag{9}$$

where α is the half angle of the nozzle, taken as 15° here. With a throat diameter of 100 μm, Mach 5 exit velocity, and the baseline pressure and temperature (40 kPa, 600 K), L/D* = 4. The exit diameter is thus 313 μm. These aspect ratios are well within the capabilities of modern micromachining systems. Thus, though ET performance may not be as high as other methods, the simplicity and easy of fabrication and operation leads ET acceleration to be a dominate candidate for microplasma based thrusters, as demonstrated by the current field of research.

B. Electrostatic

ES acceleration, best represented by ion engine grids, accelerates ions with a large electric field to high velocities. The primary advantage of ES over ET is the decoupling of the acceleration energy from the flow thermodynamics, thus making high specific impulse possible. A baseline performance calculation can be obtained by modeling the 3MT as a small ion engine and using the equations for ion engines performance such as the ones presented by Goebel.[48] The thrust for an ion engine is calculated from

$$T = \gamma\left(\dot{m}_i v_i + \dot{m}_n v_n\right) \tag{10}$$

where γ is a plume divergence factor, $\dot{m}_i$ and $\dot{m}_n$ are the ion and neutral exit mass flows respectively, and v_i and v_n are the ion and neutral exit velocities respectively. We will assume neutrals have a negligible velocity and thus do not contribute to the thrust. If ions have negligible velocity in the discharge chamber, then the ion velocity through the grids is

$$v_i = \sqrt{\frac{2eV_b}{m_i}} \qquad (11)$$

where e is the elementary charge, and V_b is the ion beam voltage. The beam voltage will be taken as equal to the anode voltage. The ion mass flow rate can be calculated from the beam current I_b from

$$\dot{m}_i = \frac{m_i}{e} I_b \qquad (12)$$

The beam current is dependent on the current flux from the plasma into the screen grid sheath and through the grid holes,

$$I_b = T_s j_i A_g \ . \qquad (13)$$

Here T_s is the screen grid transparency, j_i is the ion current density to the sheath, and A_g is the screen grid area. The ion current density is calculated from the Bohm sheath criterion

$$j_i = j_{bohm} = 0.61 e n_o \left(\frac{k_b T_e}{m_i}\right)^{1/2} \ . \qquad (14)$$

The current density has an upper limit defined by the Child-Langmuir law

$$j_{max} = \frac{4\varepsilon_o}{9} \left(\frac{2e}{m_i}\right)^{1/2} \frac{V_{accel}^{3/2}}{d^2} \qquad (15)$$

where d is taken as the distance between the grids, and the V_{accel} is the total voltage between the screen and acceleration grids. Ion engines are typically design to operate under the space charge limited current. Combining these equations, the thrust is calculated as

$$T = \gamma \left(0.61 n_o T_s A_g \eta_o \sqrt{2 e k_b T_e V_b}\right) \ , \qquad (16)$$

with the assumption that we are operating under the space-charge limit. If the current density from Eq. (14) exceeds j_{max}, then j_{max} should be used to calculate the thrust. From the equation it's shown that the thrust is independent of the propellant species mass, at least from this simple analysis. I_{SP} is calculated from

$$I_{SP} = \sqrt{\frac{2eV_b}{m_i g_o^2}} \ . \qquad (17)$$

To analyze the 3MT with electrostatic grids, we will start by assuming the thruster only has two grids, a screen grid and acceleration grid. The grid area is sized to be 125% of a circle with radius $\lambda/4$. The choice of 25% extra area is arbitrary, but attempts to account for the fact the actual microplasma source is larger than a quarter wavelength circle. The screen grid is assumed to have a 66% transparency with 2 mm diameter holes. The grids have a separation distance of 1 mm. Again argon propellant is assumed. For a 900 MHz signal in ceramic-Teflon dielectric, $\lambda/4 = 2.61$ cm, thus the grid area is 26.75 cm^2. The anode voltage is set at 600 V, screen voltage at 570 V, and acceleration grid voltage at -130 V. This gives an acceleration potential of 700 V. The voltages are set to provide a net-to-total voltage ratio $R = V_D / \left(V_s + |V_a|\right)$ between 0.8 and 0.9 for long optics lifetime as discussed by Goebel[48]. Higher voltages are possible, but may be difficult to achieve for small satellites and may lead to field breakdown between the grids.

Microplasma produced by the source will have a low electron temperature, taken as 1 eV for this analysis. The plasma density for these sources is typically around 10^{18} cm^{-3} when measured at or near the electrode gap. When allowed to expand into a larger volume discharge chamber, the density can be expected to drop by at least one order of magnitude. Thus n_o will be taken as 1 x 10^{17} m^{-3}. For the ideal case of no plume divergence ($\gamma = 1$), the thruster will produce 0.6 mN of thrust and 5500 second of I$_{SP}$. Table 1 gives additional values obtained for the current density and beam currents. The calculated current density is at ~30% of the maximum space-charge limit. Power is obtained as a product of the beam current and discharge voltage. It should be noted many details of grid optics such as ion interception and perveance are not considered here. With losses due to divergences and imperfect ion optics, the actual thrust would be half or even smaller. This analysis does provide reasonable performance parameters to allow comparison.

Table 1. Results of the electrostatic analysis.

j_{max}	49.1 A/m^2
j_i	15.12 A/m^2
I_b	0.027 A
T	0.6 mN
I_{SP}	5500 sec
Power	13 W

Performance aside, there are some practical considerations for a grid based 3MT. The first is the necessity of a neutralizing cathode. As the grids only accelerate ions, an external electron source is necessary for plume neutralization. The standard neutralizer used on ion engines is a hollow cathode. For the 3MT however, the beam current is less than 30 mA, and a hollow cathode neutralizer would add unnecessary mass and complexity. A better alternative is a simple heated filament neutralizer such as that used on the field-emission electric propulsion thruster developed by Alta.[49] It is however still an additional component that is subject to failure. The second issue to consider is the possibility of field breakdown between the grids. This is of concern for the 3MT as microplasmas typically run at higher pressures than ion engines. In the ET section a pressure of 40 kPa (300 Torr) was assumed. At a grid separation of 1 mm, the Paschen breakdown voltage at this pressure is ~1000 V for DC parallel plates. The grid holes and the addition of microwave radiation will further reduce this breakdown voltage. It is thus fair to say electric breakdown between the grids is likely for the proposed 700 V acceleration potential in the 3MT. Breakdown can be avoided by increasing the operating pressure or the grid separation. However, operation at high pressure would be inefficient because of increased ion losses and charge-exchange collisions. Increased grid separation would require higher voltages to establish proper alignment of the optics, which may exacerbate the breakdown problem. The small scale of the 3MT also means a large surface area to volume ratio, which will increase ion loss to the wall, which decreases efficiency. Even though ES can provide very high I$_{SP}$, based on the various practical issues that may prevent hamper operation, ES acceleration for microplasma is complicated and difficult to achieve, thus is not currently recommend.

C. Electromagnetic

There are two types of EM acceleration: Lorentz force acceleration of the entire plasma volume, or the use of magnetic nozzles to convert radial velocity to axial velocity. The most prominent EM thrusters are of the former type and include the magnetoplasmadynamic thruster (MPDT)[50], the pulsed inductive thruster (PIT)[51], and the pulsed plasma thruster (PPT)[52]. J x B acceleration typically requires the generation of high magnetic fields and currents to achieve decent thrust. For small satellites, PPTs are the current forerunner in EM thrusters. PPTs use gas, liquid, or solid propellants with solids such as Teflon being the most popular. All PPTs consist of a pair of conducting electrodes across which a high amplitude current pulse is driven. The current pulse ionizes the medium which creates a conducting path between the electrodes. The generated current creates a perpendicular self-field that accelerates the plasma volume to produce thrust.

An EM 3MT most resembles a gas fed PPT. In a gas feed PPT, a gaseous propellant (e.g., argon[53], or even water vapor[54]) is feed into the discharge chamber in bursts where it is quickly ionized by a spark discharge. A current is then driven through the plasma creating a current sheet and self-generated magnetic field that accelerates the plasma. The discharge chamber can take various shapes from parallel to coaxial electrodes. For the 3MT, a potential design follows the coaxial gas fed PPT by Ziemer[55]. Unfortunately, simple analytical performance models for EM thruster are rare. Choueiri developed a scaling law for MPDs that fits experimental data remarkably well.[56] However those relations are not applicable to small scale devices as the thrust increases exponentially at currents below 1000 A.

Ziemer developed numerical scaling laws for small (~10 cm outer diameter) gas fed PPTs.[55,57] The scaling laws use various parameters such as circuit inductance and capacitance that cannot be readily determined without experimental results. Ziemer's model may be the most appropriate for analysis of an EM 3MT however, and is the subject of continued work.

Some parallels can be drawn from similar pulsed thrusters. Ziemer's gas fed PPT was a coaxial device with an outer diameter of 7.25 cm, slightly larger than the 6 cm 3MT proposed here. The PPT's highest performance on argon was an impulse bit of 32 μNs at 1 μg/pulse. The current pulse peaked at 12 kA, lasted 274 μs, had an energy of 5 J per pulse, and required 200 W of steady-state power.[53] The measured I_{SP} was over 15,000 sec. The high current combined with the high power requirement would make the 3MT unusable by current or near term nanosat whose power is limited. A lower current and voltage power unit such as that used by Zhuang et. al. on the μCAT may provide a viable solution. The μCAT power unit discharges 40 A at 50 V in 0.4 ms pulses.[58] A similar inductively A EM 3MT would operate akin to a gas feed PPT, albeit at much lower current levels, and thereby lower thrust and specific impulse.

Even without performance analysis, some aspects of EM acceleration can be considered. A key question of an EM 3MT is whether to operate in steady state or pulsed mode. Most modern EM thrusters are pulsed thrusters as the high currents needed for efficient operation can be easily achieved with capacitor discharges. The 3MT could potentially be operated in both steady and pulsed modes. Steady state operation would function at lower steady currents, and generate a small self-field, thus requiring an external magnetic field. Pulsed operation may be able to operate without an external magnetic field as large current from capacitor discharges will be able to generate a significant self-field. However potential practical difficulties include material erosion due to high temperature and spot heating. Surface erosion and damage is a potential lifetime limiter. However, past research indicates lifetime is more likely to be determined by valve and switch failures before thruster body failure. Modern flight qualified and experimental PPTs have demonstrated repeated firings over 100,000 shots without failure.[52]

An EM thruster provides a simple and robust design comparable to the ET version, and much simpler than an ES thruster. The need for a neutralizer cathode is removed, and issues with electric breakdown between the grids and ion losses due to high gas density are avoided. In fact, electrical breakdown of a high density gas may be desirable in an EM 3MT. The thrust of an EM thruster can also be tailored via gas density and discharge current. While there are potential difficulties in EM acceleration of microplasmas, none are seen as true "show stoppers" and is worth further investigation.

V.   Conclusion

A proposed microthruster based on microstrip plasma resonator research is discussed. Microplasmas are an interesting regime of small scale plasmas that exhibits useful properties such as high plasma and power densities at very low power levels. Current microplasmas based propulsion includes a handful of microcavity discharge thrusters and microwave based microplasma thrusters. All utilized electrothermal acceleration where the microplasma functions as a heat source. The three acceleration types, electrothermal, electrostatic, and electromagnetic were briefly examined to estimate a performance if possible along with practical consideration. ET and ES acceleration from a simple analysis can produce the same level thrust, 0.5 and 0.6 mN respectively, but drastically different I_{SP} of 75 and 5500 sec, respectively. The ET performance is more likely to be realistic as comparison of the 1D nozzle results with experimental measurements by Takao showed good agreement. The ES calculations assumed no losses. An EM performance analysis was not performed, but Lorentz force acceleration shows potential and will be investigated further. This work suggests an ET 3MT is the simplest, though low performing design; while an EM 3MT may provide the best performance, but requires further investigation.

Table 2. Comparison of the different acceleration mechanisms. The ES power does not include additional power required for a neutralizing cathode, thus the plus. EM performance values are not available.

	ET	ES	EM
Power	1-5 W	13 + W	?
T	0.5 mN	0.6 mN	?
I_{SP}	70 sec	5500 sec	?
Complexity	Low	High	?

References

[1] Senatore, P., Klesh, A., Zurbuchen, T. H., Mckague, D., and Cutler, J., "Concept , Design , and Prototyping of XSAS : A High Power Extendable Solar Array for CubeSat Applications,"Proceedings of the 40th Aerospace Mechanisms Symposium,2010,pp. 431–444.

[2] Parker, J., Thunnissen, D., Blandino, J., and Ganapathi, G., "The preliminary design and status of a hydrazine milliNewton thruster development," *35th Joint Propulsion Conference and Exhibit*, American Institute of Aeronautics and Astronautics, 1999.

[3] Teasdale, D., Milanovic, V., Chang, P., and Pister, K. S. J., "Microrockets for smart dust," *Smart Materials and Structures*, vol. 10, Dec. 2001, pp. 1145–1155.

[4] Takao, Y., and Ono, K., "A miniature electrothermal thruster using microwave-excited plasmas: a numerical design consideration," *Plasma Sources Science and Technology*, vol. 15, 2006, p. 211.

[5] Zhuang, T., Shashurin, A., Chiu, D., Teel, G., and Keidar, M., "Micro-Cathode Arc Thruster Development and Characterization,"32nd International Electric Propulsion Conference,2011,pp. IEPC–2011–266.

[6] Rayburn, C. D., Campbell, M. E., and Mattick, a. T., "Pulsed Plasma Thruster System for Microsatellites," *Journal of Spacecraft and Rockets*, vol. 42, Jan. 2005, pp. 161–170.

[7] Conversano, R., and Wirz, R., "CubeSat Lunar Mission Using a Miniature Ion Thruster," *47th AIAA/ASME/SAE/ASEE Joint Propulsion Conference & Exhibit*, American Institute of Aeronautics and Astronautics, 2011.

[8] Mariotti, D., and Sankaran, R. M., "Microplasmas for Nanomaterials Synthesis," *Journal of Physics D, Applied Physics*, vol. 43, 2010.

[9] Mariotti, D., "Nonequilibrium and effect of gas mixtures in an atmospheric microplasma," *Applied Physics Letters*, vol. 92, 2008, p. 151505.

[10] Belostotskiy, S. G., Khandelwal, R., Wang, Q., Donnelly, V. M., Economou, D. J., and Sadeghi, N., "Measurement of electron temperature and density in an argon microdischarge by laser Thomson scattering," *Applied Physics Letters*, vol. 92, 2008, p. 221507.

[11] Iza, F., Lee, J. K., and Kong, M. G., "Electron Kinetics in Radio-Frequency Atmospheric-Pressure Microplasmas," *Physical Review Letters*, vol. 99, Aug. 2007, pp. 2–5.

[12] Choi, J., Iza, F., Lee, J. K., and Ryu, C.-M., "Electron and Ion Kinetics in a DC Microplasma at Atmospheric Pressure," *IEEE Transactions of Plasma Science*, vol. 35, 2007.

[13] Yanguas-Gil, A., Focke, K., Benedikt, J., and von Keudell, A., "Optical and electrical characterization of an atmospheric pressure microplasma jet for Ar/CH4 and Ar/C4H4 mixtures," *Journal of Applied Physics*, vol. 101, 2007, p. 103307.

[14] White, A. D., "New Hollow Cathode Glow Discharge," *Journal of Applied Physics*, vol. 30, 1959, p. 711.

[15] Frame, J. W., Wheeler, D. J., DeTemple, T. a., and Eden, J. G., "Microdischarge devices fabricated in silicon," *Applied Physics Letters*, vol. 71, 1997, p. 1165.

[16] Papadakis, A. P., Rossides, S., and Metaxas, A. C., "Microplasmas : A Review," 2011, pp. 45–63.

[17] Eden, J. G., and Park, S.-J., "Microcavity Plasma Devices and Arrays: A New Realm of Plasma Pysics and Photonic Applications," *Plasma Physics and Controlled Fusion*, vol. 47, 2005, p. B83.

[18] Eden, J. G., and Park, S.-J., "New opportunities for plasma science in nonequilibrium, low-temperature plasmas confined to microcavities: There's plenty of room at the bottom," *Physics of Plasmas*, vol. 13, 2006, p. 057101.

[19] Foest, R., Schmidt, M., and Becker, K., "Microplasmas, an emerging field of low-temperature plasma science and technology," *International Journal of Mass Spectrometry*, vol. 248, Feb. 2006, pp. 87–102.

[20] Chen, J., Park, S.-J., Fan, Z., Eden, J. G., and Liu, C., "Development and Characterization of Micromachined Hollow Cathode Plasma Display Devices," *Journal of Microelectromechanical Systems*, vol. 11, 2002, pp. 536–543.

[21] Shimizu, Y., Sasaki, T., Ito, T., Terashima, K., and Koshizaki, N., "Fabrication of Spherical Carbon via UHF Inductively Coupled Microplasma CVD," *Journal of Physics D, Applied Physics*, vol. 36, 2003, pp. 2940–2944.

[22] Iza, F., and Hopwood, J. A., "Low-Power Microwave Plasma Source Based on a Microstrip Split-Ring Resonator," *IEEE Transactions of Plasma Science*, vol. 31, 2003, pp. 782–787.

[23] Schermer, S., Bings, N., and Bilgiç, A., "An improved microstrip plasma for optical emission spectrometry of gaseous species," *Spectrochimica Acta B: Atomic Spectroscopy*, vol. 58, 2003, pp. 1585–1596.

[24] Ichiki, T., "Localized and ultrahigh-rate etching of silicon wafers using atmospheric-pressure microplasma jets," *Journal of Applied Physics*, vol. 95, 2004, p. 35.

[25] Chang, F.-C., Richmonds, C., and Sankaran, R. M., "Microplasma-Assisted Growth of Colloidal Ag Nanoparticles for Point-of-Use Surface-Enhanced Rama Scattering Applications," *Journal of Vacuum Science & Technology A*, vol. 28, 2010, p. L5.

[26] Park, S.-J., Chen, K.-F., Ostrom, N. P., and Eden, J. G., "40000 Pixel Arrays of Ac-Excited Silicon Microcavity Plasma Devices," *Applied Physics Letters*, vol. 86, 2005, p. 111501.

[27] Karanassios, V., "Microplasmas for chemical analysis : analytical tools or research toys ?," vol. 59, 2004, pp. 909–928.

[28] Kim, S. J., Chung, T. H., Bae, S. H., and Leem, S. H., "Induction of apoptosis in human breast cancer cells by a pulsed atmospheric pressure plasma jet," *Applied Physics Letters*, vol. 97, 2010, p. 023702.

[29] Penache, C., Miclea, M., Bräuning-Demian, A., Hohn, O., Schössler, S., Jahnke, T., Niemax, K., and Schmidt-Böcking, H., "Characterization of a high-pressure microdischarge using diode laser atomic absorption spectroscopy," *Plasma Sources Science and Technology*, vol. 11, Nov. 2002, p. 476.

30   Burton, R. L., Eden, J. G., Park, S., Yoon, J. K., Chadenedes, M. De, and Garrett, S., "Initial Development of the Microcavity Discharge Thruster,"31st International Electric Propulsion Conference,2009,pp. IEPC–2009–169.

31   Takahashi, T., Kitanishi, S., Takao, Y., Eriguchi, K., and Ono, K., "Microwave-excited microplasma thruster: design improvement for implementation to satellite," *31st International Electric Propulsion Conference*, vol. IEPC-2009-, 2009.

32   Guangquing, X., Genwang, M., Maolin, C., and Chuijie, W., "Theoretical and Experimental Investigation of Microhollow Chathode Discharge for the Application to Micro Plasma Thrusters,"31st International Electric Propulsion Conference,2009,pp. IEPC–2009–028.

33   Hitomi, R., Kobayashi, N., Asanuma, K., Horisawa, H., and Funaki, I., "Thrust Performance of a Micro-Multi-Plasmajet-Array Thruster,"32nd International Electric Propulsion Conference,2011,pp. IEPC–2011–289.

34   Kothnur, P. S., and Raja, L. L., "Simulation of Direct-Current Microdischarges for Application in Electro-Thermal Class of Small Satellite Propulsion Devices," *Contributions to Plasma Physics*, vol. 47, Feb. 2007, pp. 9–18.

35   Tuyen, P. D., and Shin, J., "Experimental investigation of micro plasma thruster for a microscale spacecraft propulsion system,"International Forum on Strategic Technology,2010,pp. 59–62.

36   Kawanabe, T., Takahashi, T., Takao, Y., Eriguchi, K., and Ono, K., "Microwave-excited Microplasma Thruster with Applied Magnetic Field,"32nd International Electric Propulsion Conference,2011,pp. IEPC–2011–262.

37   Choueiri, E., and Polzin, K., "Faraday acceleration with radio-frequency assisted discharge (FARAD),"40th AIAA Joint Propulsion Conference,2004.

38   Williams, L. T., "Ion Acceleration Mechanisms of Helicon Thrusters Ion Acceleration Mechanisms of Helicon Thrusters," Ph.D. Thesis, Aerospace, Georgia Institute of Technology, Atlanta, GA, 2013.

39   Peterson, P. Y., Massey, D., Shabshelowitz, A., Shastry, R., and Liang, R., "Performance and Plume Characterization of a Helicon Hall Thruster,"32nd International Electric Propulsion Conference,2011.

40   Bilgic, A. M., Engel, U., Voges, E., Kuckelheim, M., and Broekaert, J. A. C., "A New Low-Power Microwave Plasma Source Using Microstrip Technology for Atomic Emission Spectrometry," *Plasma Sources Science and Technology*, vol. 9, 2000.

41   Iza, F., and Hopwood, J., "Split-ring resonator microplasma: microwave model, plasma impedance and power efficiency," *Plasma Sources Science and Technology*, vol. 14, May 2005, pp. 397–406.

42   Miura, N., and Hopwood, J., "Spatially resolved argon microplasma diagnostics by diode laser absorption," *Journal of Applied Physics*, vol. 109, 2011, p. 013304.

43   Zhu, X.-M., Chen, W.-C., and Pu, Y.-K., "Gas temperature, electron density and electron temperature measurement in a microwave excited microplasma," *Journal of Physics D: Applied Physics*, vol. 41, May 2008, p. 105212.

44   Miura, N., and Hopwood, J., "Internal structure of 0.9 GHz microplasma," *Journal of Applied Physics*, vol. 109, 2011, p. 113303.

45   Günther-Schulze, A., "Die Stromdichte des normalen Kathodenfalles," *Zeitschrift für Physik*, vol. 19, 1923, pp. 313–332.

46   Schoenbach, K. H., Verhappen, R., Tessnow, T., Peterkin, F. E., and Byszewski, W. W., "Microhollow cathode discharges," *Applied Physics Letters*, vol. 68, 1996, p. 13.

47   Takao, Y., Eriguchi, K., and Ono, K., "A miniature electrothermal thruster using microwave-excited microplasmas: Thrust measurement and its comparison with numerical analysis," *Journal of Applied Physics*, vol. 101, 2007, p. 123307.

48   Goebel, D. M., and Katz, I., *Fundamentals of Electric Propulsion: Ion and Hall Thrusters*, Pasadena: Jet Propulsion Laboratory, 2008.

49   Marcuccio, S., Nicolini, D., and Saviozzi, M., "Endurance test of the micronewton FEEP thruster,"36th AIAA Joint Propulsion Conference,2000.

50   Choueiri, E. Y., Ziemer, J. K., and Propulsion, E., "Quasi-Steady Magnetoplasmadynamic Thruster Performance Database," *Journal of Propulsion and Power*, vol. 17, Sep. 2001, pp. 967–976.

51   Polzin, K. a., "Comprehensive Review of Planar Pulsed Inductive Plasma Thruster Research and Technology," *Journal of Propulsion and Power*, vol. 27, May 2011, pp. 513–531.

52   Molina-Cabrera, P., Herdrick, G., Lau, M., and Fausolas, S., "Pulsed Plasma Thrusters: a worldwide review and long yearned classification,"32nd International Electric Propulsion Conference,2011,pp. IEPC–2011–340.

53   Ziemer, J., and Cubbin, E., "Performance characterization of a high efficiency gas-fed pulsed plasma thruster,"33rd Joint Propulsion …,1997,pp. 1–12.

54   Ziemer, J., and Petr, R., "Performance of gas fed pulsed plasma thrusters using water vapor propellant,"38th AIAA Joint Propulsion Conference & Exhibit, …,2002,pp. 1–8.

55   Ziemer, J. K., "Performance Scaling of Gas-Fed Pulsed Plasma Thrusters," Princeton University, 2001.

56   Choueiri, E., "On the thrust of self-field MPD thrusters,"25 thInternational Electric Propulsion Conference, …,1997,pp. IEPC–97–121.

57   Ziemer, J. K., and Choueiri, E. Y., "Scaling laws for electromagnetic pulsed plasma thrusters," *Plasma Sources Science and Technology*, vol. 10, Aug. 2001, pp. 395–405.

58   Zhuang, T., Shashurin, a, Keidar, M., and Beilis, I. I., "Circular periodic motion of plasma produced by a small-scale vacuum arc," *Plasma Sources Science and Technology*, vol. 20, Feb. 2011, p. 015009.